

Influence of material gradation on the stress behavior of functionally graded beams: analysis and modeling

Benferhat Rabia^{1,2}, Tahar Hassaine Daouadji^{*1,2}, Abdelaziz Hadj Henni¹

¹Department of Civil Engineering, Ibn Khaldoun University of Tiaret, Algeria

²Laboratory of Geomatics and Sustainable Development LGéo2D, University of Tiaret, Algeria

(Received July 28, 2025, Revised February 25, 2026, Accepted February 27, 2026)

Abstract. This paper investigates the plane stress behavior of a cantilever beam made of functionally graded material (FGM) subjected to combined shear and bending loading. A new formulation of the elastic modulus of FGM materials is proposed, incorporating two gradation parameters: the first representing the material gradation and the second the ratio of the longitudinal elastic modulus. Three models of the mechanical property distribution through the beam thickness are considered: the classical variation, the new model-1, and the new model-2. The mathematical formulation, based on the static equilibrium equations, is developed to predict the distribution of stresses and displacements in the beam subjected to a tangential force applied at its free end. The influence of the gradation parameters k_1 , k_2 and the length-to-thickness ratio L/h on the stress and displacement response is also analyzed.

Keywords: cantilever beam; material gradation; shear and bending loading; static analysis

1. Introduction

Advanced composite materials known as functionally graded materials (FGMs) exhibit a progressive change in their mechanical characteristics, usually in one or more spatial directions. By decreasing stress concentrations and improving resistance to mechanical and thermal loads, this constant fluctuation makes it possible to optimize structural performance. Beams are among the various structural components composed of FGMs that are essential to practical engineering applications, including mechanical components (machine beams, shafts), and aerospace structures (wing spars, fuselage elements). The structural behavior of functionally graded material (FGM) beams under varied mechanical and thermal loading conditions has been the subject of numerous studies. To precisely capture the impact of material gradation and structural configuration, these studies use both analytical and numerical techniques. Reddy [1] laid the groundwork for more accurate modeling of FG structures by creating a modified Timoshenko beam theory that takes transverse shear deformation into account without the requirement for a correction factor. Building on this, Chakraborty [2] investigated thermoelastic reactions in FG beams using a super-convergent finite element based on first-order shear deformation theory (FSDT). Similar issues were addressed by Kadoli et al. in a related study using comparative formulations. Rizov [3]

*Corresponding author, Professor, E-mail: daouadjitahar@gmail.com

developed four analytical modeling methods for FG beams, showing enhanced accuracy for both static and dynamic assessments. These methods included a Fourier-Galerkin method, a higher-order shear deformation theory, and two equivalent single-layer models. Later, Simsek [4] used improved beam models in the modified couple stress theory to investigate the stability, free vibration, and static response of micro-scale FG beams [5-20]. Regarding elasticity solutions, Sankar [21] offered a closed-form solution for simply supported beams under sinusoidal stress that was based on Euler-Bernoulli theory. Using Airy's stress function, Zhong and Yu [22] developed a two-dimensional elasticity solution for cantilever FG beams. In their one-dimensional static analysis of FG structures, Filippi [23] used the Carrera Unified Formulation (CUF), which allowed for flexibility in the selection of kinematic assumptions. Thermal and vibrational behaviors under more complicated conditions have been studied in recent contributions. Alimoradzadeh [24] investigated the nonlinear free vibration of FG beams on nonlinear viscoelastic foundations under uniform thermal fields, while Adim [25] investigated the thermal bending of sandwich FG beams using a shear deformation technique. Bennai [26] addressed buckling and free vibration of imperfect porous FG beams using a higher-order shear deformation theory.

A number of authors have included extensive numerical techniques or artificial intelligence into their modeling. The vibrational and buckling responses of edge-cracked FG beams were investigated by Yaylacı [27] utilizing multilayer perceptron networks in conjunction with the finite element approach. In order to analyze FG Timoshenko beams under hydrothermal loading and resting on silica aerogel foundations, Khorasani [28] presented a novel refined model that is independent of the porosity index. Using a quasi-3D formulation, Youcef [29] examined the effect of porosity distribution on the free vibration behavior of FG microbeams in terms of three-dimensional and quasi-3D theories. Guendouz [30] successfully captured edge effects in their coupled torsion-bending analysis of composite open-section FG beams using the three-dimensional Saint-Venant solution. Saghafi [31] made another noteworthy contribution by employing two-dimensional elasticity theory to examine the static and vibrational responses of sandwich beams with FG cores and viscoelastic surfaces. Hosseini [32] applied geometric deepness effects and nonlocal elasticity to the in-plane free vibration of curved FG nanobeams. Candaş [33] investigated crack propagation in functionally graded materials (FGMs) containing micro-cracks using ordinary state-based Peridynamic theory. The study focused on the dynamic fracture behavior, based on the Kalthoff-Winkler experiment. Siam [34] presented closed-form solutions for viscoelastic FG nanobeams embedded in elastic media using the nonlocal differential form of Eringen's theory. Candaş [35] used bond-based Peridynamics to investigate dynamic crack propagation in functionally graded materials (FGMs) with micro-cracks. The results showed that cracks propagated more slowly and toughness increased in harder regions. Bouazza [36] investigated the post-buckling response of FG beams under basic boundary conditions in the context of nonlinear stability. Hacıoğlu [37] investigated large deflections of cantilever beams made of nonlinearly elastic, modified Ludwick-type functionally graded materials (FGMs) using finite element analysis (FEA). The results showed that both the material gradient and the number of laminae significantly influenced the normal stress distribution along the beam as well as its vertical and horizontal deflections. Lastly, Kablia [38] extended the field of fracture mechanics in gradient materials by investigating the effects of spatial translational motion on longitudinal fracture behavior in FG beams with nonlinear elastic properties.

Recent research on functionally graded (FG) structures has focused on understanding the effects of material gradation, porosity, and complex environmental loads on their mechanical behavior. Several studies have addressed dynamic and static responses of FG beams, plates, and

shells under thermal, hygro-thermal, and mechanical excitations. For instance, Youzera [39] analyzed free vibration of porous FGM beams under thermal loading, while Benhenni [40] studied dynamic behavior of porous FG spherical shells, highlighting the influence of homogenization models. Other works have explored advanced FG plates reinforced with carbon nanotubes and porous FG plates under bending and hygro-thermo-mechanical loads [41, 42]. The impact of imperfections, graded patterns, and viscoelastic foundations on FG beams and plates has also been investigated [42], showing significant effects on stress distribution, deflections, and stability. Moreover, recent studies by [43, 44] emphasize the combined influence of boundary conditions, porosity distribution, and thermal environments on the performance of FG plates and sandwich structures.

Functionally graded material (FGM) beams are now mostly studied using traditional gradation profiles, where the material properties usually differ from the top surface to the bottom surface. Adopting a different distribution, in which characteristics change from the material's outer surface toward its inner area, offers a more accurate and pertinent simulation of the structural behavior in many real-world scenarios. In this study investigate the elastic behavior of cantilever beams made of bigraded functionally graded materials (FGMs) subjected to transverse shear loads. An analytical approach, based on elasticity theory, is developed to determine the stress and deformation distributions within the beam. The mechanical properties of the material, particularly Young's modulus, are assumed to vary continuously according to two types of gradation laws: a conventional model and a newly proposed one. Closed-form analytical expressions for the stress fields are derived for these bigraded FGM beams under shear, enabling the analysis of the influence of different gradation patterns on the mechanical response of cantilever beams.

2. Theoretical formulations

This section presents the theoretical formulation used to analyze the mechanical behavior of functionally graded cantilever beams under transverse shear loading. The model is based on elasticity theory and considers the continuous variation of material properties through the beam thickness, including both conventional power-law and newly proposed bigraded distributions. The governing relations for Young's modulus variation and the associated kinematic assumptions are introduced as the basis for the subsequent analytical developments.

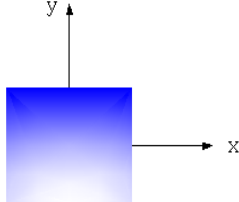
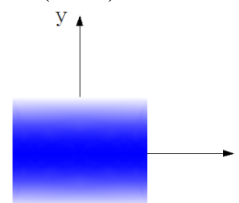
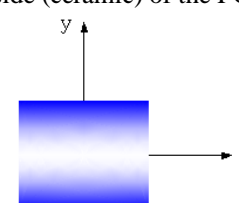
2.1 Functionally graded beam

This study investigates an elastic cantilever beam made of functionally graded material (FGM), composed of ceramic and metal, with distinct material properties such as Young's modulus and Poisson's ratio. The material properties vary continuously along the thickness direction, with Poisson's ratio assumed to be constant, while Young's modulus follows a power-law distribution (P-FGM). To describe this gradation, a power-law function is adopted and further generalized by introducing two independent parameters: k_1 , representing the material gradation, and k_2 , representing the longitudinal elastic modulus ratio. The Young's modulus of aluminum is denoted by E_2 [45].

$$E(y) = E_2[(k_2 - 1)v(y) + 1] \quad (1)$$

The Young's modulus for aluminum is denoted by E_2 , while k_1 and k_2 represent the material

Table 1. Geometries of FGM Beams and the Corresponding Mixing Laws

models	Form of mechanical property distribution	(E) and (ρ)
Classical model	 <p>Figure 1(a). Variation from the top (ceramic) to the bottom (metal) of the FG beam</p>	$E(y) = E_2 \left[(k_2 - 1) \left(\frac{y}{h} + \frac{1}{2} \right)^{k_1} + 1 \right]$
New model-1	 <p>Figure 1(b). Variation from the outside (metal) to the inside (ceramic) of the FG beam</p>	$E(z) = E_2 \left[(k_2 - 1) \left(1 - 2 \frac{ y }{h} \right)^{k_1} + 1 \right]$
New model-2	 <p>Figure 1(c). Variation from the outside (ceramic) to the inside (metal) of the FG beam</p>	$E(z) = E_1 \left[\left(\frac{1}{k_2} - 1 \right) \left(1 - 2 \frac{ y }{h} \right)^{k_1} + 1 \right]$

gradation and the longitudinal elastic modulus ratio, respectively.

The volume percentage $V(y)$, which characterizes the material gradation in conventional FGM beams, ensures a gradual variation of the mechanical properties from the top to the bottom surface of the beam. The volume fraction for a classical power-law FGM beam can be written as follows [45]:

$$V(y) = \left(\frac{y}{h} + \frac{1}{2} \right)^{k_1} \quad (2)$$

The volume fraction $V(y)$ represents the local proportion of one constituent material (e.g., ceramic) in a functionally graded material (FGM) beam at a given position y through the thickness. k_1 is the power-law index that controls the material gradation profile.

Substituting Eq. (2) into Eq. (1) yields the expression for the Young's modulus of a classical FGM beam [45]:

$$E(y) = E_2 \left[(k_2 - 1) \left(\frac{y}{h} + \frac{1}{2} \right)^{k_1} + 1 \right] \quad (3)$$

This study proposes a novel method of material property variation through the FGM beam's thickness, where the gradation takes place from the outer surface in the direction of the inner

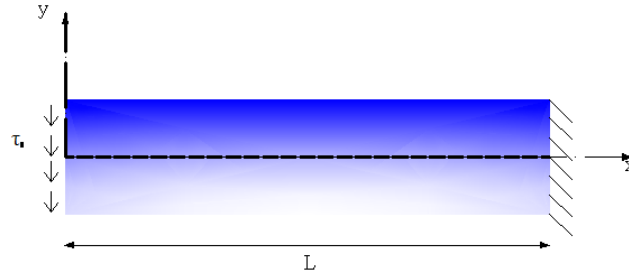


Figure 2. The FG cantilever beam's geometry under shear load

surface. The expression for this new gradation is:

$$V(y) = \left(1 - \frac{2|y|}{h}\right)^{k_1} \quad (4)$$

In this case, the new formula $V(y)$ ensures a gradual variation of the mechanical properties from the FGM beam's outer surface to its inner surface. As a result, the new model-1's Young's modulus is determined by:

$$E(y) = E_2 \left[(k_2 - 1) \left(1 - \frac{2|y|}{h}\right)^{k_1} + 1 \right] \quad (5)$$

Model-1 assumes that the inside portion of the beam is ceramic and the exterior portion is made of metal. On the other hand, model-2 has metal on the inside and ceramic on the outside. Thus, the Young's modulus for model-2 can be written as follows:

$$E(y) = E_1 \left[(k_2 - 1) \left(1 - \frac{2|y|}{h}\right)^{k_1} + 1 \right] \quad (6)$$

The power-law index k_1 is always a positive real number ($0 \leq k_1 \leq \infty$), and y is the distance from the FGM beam's mid-plane.

2.2 Elasticity solution

A functionally graded cantilever beam of uniform thickness h is defined within a Cartesian coordinate system (Fig. 2), where the upper and lower surfaces lie at plane $y=h/2$ and $-y=h/2$, respectively. The beam extends along the directions L and b , and a plane stress condition is assumed in the x - y plane. The material properties vary continuously through the thickness of the beam, either from the top surface to the bottom surface or from the outer surface toward the inner region, depending on the type of gradation adopted.

The equilibrium equations, in the absence of body forces, are expressed as:

$$\frac{\partial \sigma_x}{\partial x} + \frac{\partial \tau_{xy}}{\partial y} = 0 \quad (7a)$$

$$\frac{\partial \tau_{xy}}{\partial x} + \frac{\partial \sigma_y}{\partial y} = 0 \quad (7b)$$

where σ_x , σ_y , τ_{xy} are stress components.

It is determined that the normal stress in the y-direction is zero ($\sigma_y = 0$) based on the boundary conditions applied to the beam's upper and lower (unloaded) surfaces. The equilibrium Eq. (7) can be integrated to provide the following stress expressions:

$$\tau_{xy} = f(y) \quad (8a)$$

$$\sigma_x = -xf'(y) + g(y) \quad (8b)$$

Where $f(y)$ and $g(y)$ are unknown functions.

The following are the relations between displacements and strains:

$$\varepsilon_x = \frac{1}{E(y)} \sigma_x, \quad (8c)$$

$$\varepsilon_y = \frac{-\nu}{E(y)} \sigma_x, \quad (8d)$$

$$\gamma_{xy} = 2 \frac{1+\nu}{E(y)} \tau_{xy} \quad (8e)$$

Where the strain components ε_x , ε_y , γ_{xy} should meet the strain compatibility equation as follows:

$$\frac{\partial^2 \varepsilon_x}{\partial y^2} + \frac{\partial^2 \varepsilon_y}{\partial x^2} - \frac{\partial^2 \gamma_{xy}}{\partial x \partial y} = 0 \quad (9)$$

The following is obtained by solving Eq. (5) and determining the unknown functions $f(y)$ and $g(y)$:

$$\left[\frac{g(y)}{E(y)} \right]'' - x \left[\frac{f'(y)}{E(y)} \right]'' = 0 \quad (10)$$

Eq. (10) leads us to the following equations:

$$g(y) = c_1 y E(y) + c_2 E(y) \quad (11a)$$

$$f'(y) = c_3 y E(y) + c_4 E(y) \quad (11b)$$

$$f(y) = c_3 \int_{-h/2}^y y E(y) dy + c_4 \int_{-h/2}^y E(y) dy + c_5 \quad (11c)$$

Where c_i : $i=1$ à 5 are constants of integration.

The following are the elasticity boundary conditions at the upper and lower surfaces:

$$\tau_{xy}(x, -h/2) = f(-h/2) = 0, \quad (12a)$$

$$\tau_{xy}(x, +h/2) = f(+h/2) = 0, \quad (12b)$$

$$c_5 = 0 \tag{12c}$$

The FGM beam's left end (free) has the following boundary conditions:

$$N_0 = 0, \tag{13a}$$

$$M_0 = 0, \tag{13b}$$

$$Q_0 = \tau_0 h \tag{13c}$$

Where the axial force, moment, and shear force at $x = 0$ are indicated by the symbols N_0 and M_0 the following are assumed to be the boundary conditions for the fixed end at the right end (fixed) of the beam:

$$u = v = 0,$$

$$\frac{\partial v}{\partial x} = 0 \quad \text{at } x = L, \quad y = 0 \tag{14a}$$

The displacement components could be obtained as follows after integrating Eq. (8):

$$u = x S_{11}g(y) - \frac{x^2}{2} S_{11}f'(y) + \int_{-h/2}^y (y - \xi) S_{12}f'(y) d\xi + \int_{-h/2}^y S_{66}f(y) d\xi - \delta y + u_0, \tag{14b}$$

$$v = \int_{-h/2}^y s_{12}g(y) d\xi - x \int_{-h/2}^y s_{12}f'(y) d\xi + \frac{c_1}{6} x^3 - \frac{c_3}{2} x^2 + \delta x + v_0 \tag{14c}$$

Where: u_0, v_0 and δ are integral constants.

The following matrix system is obtained by substituting the above equations:

$$\begin{bmatrix} \gamma_2(h/2) & \eta_2(h/2) & 0 & 0 \\ \gamma_1(h/2) & \eta_1(h/2) & 0 & 0 \\ 0 & 0 & \gamma_2(h/2) & \eta_2(h/2) \\ 0 & 0 & \gamma_1(h/2) & \eta_1(h/2) \end{bmatrix} \begin{bmatrix} c_1 \\ c_2 \\ c_3 \\ c_4 \end{bmatrix} = \begin{bmatrix} 0 \\ 0 \\ \tau_0 h \\ 0 \end{bmatrix} \tag{15}$$

With:

$$\gamma_1(h/2) = \int_{-h/2}^{+h/2} \xi E(\xi) d\xi \tag{16a}$$

$$\gamma_2(h/2) = \int_{-h/2}^{+h/2} \left(\frac{h}{2} - \xi\right) \xi E(\xi) d\xi \tag{16b}$$

$$\eta_1(h/2) = \int_{-h/2}^{+h/2} E(\xi) d\xi \tag{16c}$$

$$\eta_2(h/2) = \int_{-h/2}^{+h/2} \left(\frac{h}{2} - \xi\right) E(\xi) d\xi \quad (16d)$$

3. Results and discussion

This section presents a numerical study of a cantilever beam made of functionally graded material (FGM), with dimensions $L=1$ m and $h=0.1$ m, subjected to a tangential load of $\tau_0=108$ N/ml. The analysis, based on the static equilibrium equations, is performed for both homogeneous and P-FGM materials, considering different gradation parameters k_1 and k_2 , as well as the length-to-thickness ratio L/h . Three models of through-thickness property distribution are considered: the classical variation, new model-1, and new model-2. The gradation function follows a power-law P-FGM form, with $\nu=0.3$ and $E_2=70$ GPa for aluminum. The objective is to assess the influence of the gradation parameters, the material model, and the geometry on the stress and displacement distributions.

$$\bar{v} = \frac{10E_2\nu h^3}{\tau_0 L^4} \quad (17a)$$

$$\bar{\sigma}_x = \frac{\sigma_x}{\tau_0} \quad (17b)$$

$$\bar{\tau} = \frac{\tau_{xy}}{\tau_0} \quad (17c)$$

Table 2 presents a comparison of the displacements and stresses of a cantilever FGM beam subjected to shear loading in bending. Three models of the variation of mechanical properties through the thickness of the beam are considered, namely: the classical variation, the new model-1,

Table 2. Comparison dimensionless stress and displacement comparison for different FGM gradations in a cantilever beam

k_1	k_2	Classical	New	New	Classical	New	New	Classical	New	New
		model	Model-1	Model-2	model	Model-1	Model-2	model	Model-1	Model-2
		$\sigma_{xx}/\tau_0 (L/2; h/2)$			$\tau_{xy}/\tau_0 (L/2; 0)$			$\bar{v}(0,0)$		
0	1	29,999	29,999	29,999	1,500	1,500	1,500	-4,000	-4,000	-4,000
	2	29,999	29,999	29,999	1,500	1,500	1,500	-1,999	-1,999	-8.000
	5	29,999	29,999	29,999	1,500	1,500	1,500	-0,799	-0,799	-20.000
1	1	29,999	29,999	29,999	1,500	1,500	1,500	-4,000	-4,000	-4,000
	2	36,923	23,9999	34,285	1,499	1,600	1,428	-2,769	-3,1999	-4.571
	5	45,652	14,9999	37,500	1,499	1,7499	1,3750	-1,565	-1,9999	-5.000
2	1	29,999	29,999	29,999	1,500	1,500	1,500	-4,000	-4,000	-4,000
	2	39,252	27,2727	31,578	1,472	1,5909	1,447	-2,990	-3,6363	-4.210
	5	52,817	21,4285	32,608	1,426	1,78571	1,413	-1,972	-2,8571	-4.347

Table 3. Dimensionless stress and displacement behavior of an FGM cantilever beam with various gradation models; $k_1=2$; $k_2=5$

L/h	Classical	New	New	Classical	New	New	Classical	New	New
	model	Model-1	Model-2	model	Model-1	Model-2	model	Model-1	Model-2
	$\sigma_{xx}/\tau_0 (L/2; h/2)$			$\tau_{xy}/\tau_0 (L/2; 0)$			$\bar{v}(0,0)$		
5	26.400	10.714	16.304	1.426	1.785	1.413	-3.943	-5.714	-8.695
20	105.633	42.857	65.217	1.426	1.785	1.413	-0.985	-1.428	-2.173
50	264.084	107.142	163.043	1.426	1.785	1.413	-0.394	-0.571	-0.869

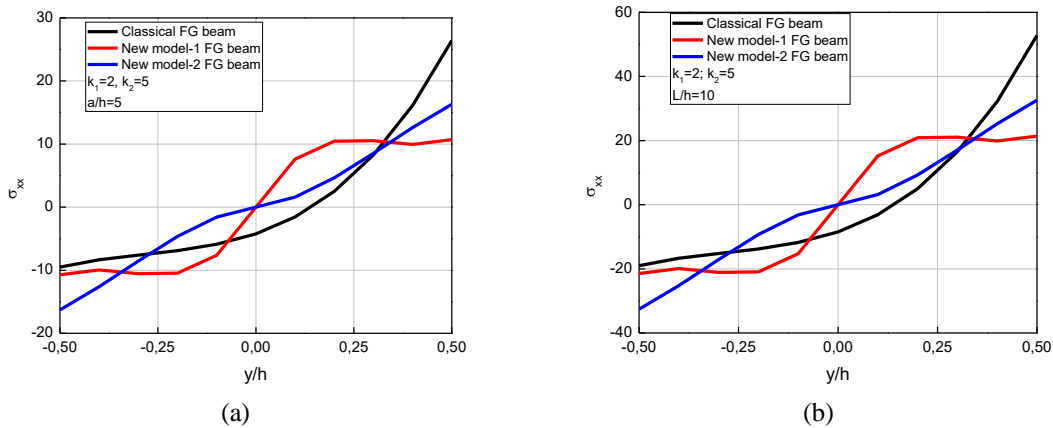


Figure 3. Normal stress σ_{xx} variation through the thickness of a cantilever FGM beam for different mechanical property variations: (a) $a/h=5$, (b) $a/h=10$

and the new model-2. The parameter k_1 takes the values 0, 1, and 2, while the parameter k_2 takes the values 1, 2, and 5. According to the results, it can be observed that the stresses and displacements remain unchanged for the different types of property variation when $k_1=0$ and $k_2=1$, $k_1=1$ and $k_2=1$, or $k_1=2$ and $k_2=1$. It is also observed that the form of variation of the mechanical properties has a significant influence on the displacements and stresses of a cantilever FGM beam under shear loading in bending.

The displacements and stresses of a cantilever FGM beam subjected to shear loading in bending, with different forms of variation of the mechanical property distribution, are also compared in Table 3 for different values of the L/h ratio ($L/h=5, 20$, and 50). It is clear that the normal stress σ_{xx} increases as the L/h ratio increases, while the displacements become smaller. It can be concluded that the shear stress τ_{xy} remains constant and that the L/h ratio does not affect τ_{xy} . The normal stress is lower for a cantilever FGM beam following the new model-1.

Fig. 3 presents a comparison of the normal stress σ_{xx} through the thickness of a cantilever FGM beam subjected to shear loading in bending. Three models of the variation of mechanical properties through the thickness of the beam are considered, namely: the classical variation, the new model-1, and the new model-2. The parameter k_1 is fixed at 2 and k_2 at 5, while the length-to-thickness ratio L/h takes the values 5 and 10. According to the results, it can be observed that the normal stress σ_{xx} increases significantly as the L/h ratio increases, while the difference between the three mechanical property models becomes more pronounced for larger L/h . It is also observed that the form of variation of the mechanical properties has a significant influence on the normal

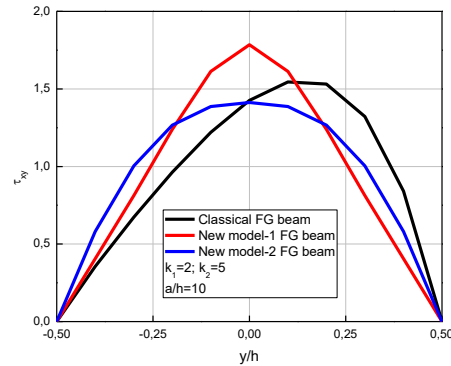


Figure 4. Shear stress τ_{xy} variation through the thickness of a cantilever FGM beam for different mechanical property variations

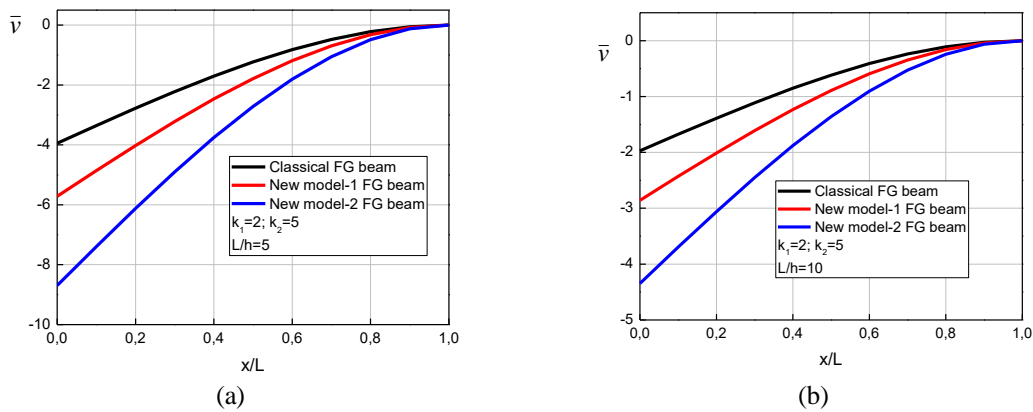


Figure 5. Variation of the normalized displacement \bar{v} along the length and at the free end of a cantilever FGM beam for different mechanical property distributions: (a) $a/h=5$, (b) $a/h=10$

stress distribution through the thickness, with the new model-1 resulting in lower σ_{xx} values compared to the classical and new model-2, especially at the upper surface of the beam.

Fig. 4 illustrates the distribution of the shear stress τ_{xy} through the thickness of a cantilever FGM beam subjected to shear loading in bending. Three models of the variation of mechanical properties through the thickness are considered: the classical variation, the new model-1, and the new model-2. The parameters k_1 and k_2 are set to 2 and 5, respectively, and the length-to-thickness ratio L/h is taken as 10. According to the results, the shear stress τ_{xy} exhibits a parabolic distribution through the thickness, with zero values at the surfaces for all three models. The maximum values are located at the mid-thickness for the new models 1 and 2, whereas they are slightly shifted toward the upper (ceramic) part for the classical model. It is also observed that the variation of mechanical properties has a slight influence on the maximum shear stress, with the new model-1 producing the highest values at the mid-thickness, followed by the classical model and the new model-2. These results indicate that the distribution of mechanical properties has a weaker effect on the shear stress than on the normal stress (Fig. 2).

Fig. 5 shows the evolution of the normalized displacement \bar{v} along the length of a cantilever FGM beam and at its free end, under shear loading in bending. The analysis considers three

different distributions of mechanical properties through the beam thickness: the classical distribution, new model-1, and new model-2. For this comparison, the parameters k_1 are set to 2 and 5, respectively, while two values of the length-to-thickness ratio L/h are examined, namely 5 and 10. According to the results, the normalized displacement \bar{v} decreases (in the negative direction) along the beam length from the clamped end ($x/L=0$) to the free end ($x/L=1$) for all three models. It can also be observed that the displacement magnitude is higher for the classical model, followed by the new model-1 and the new model-2, indicating that the distribution of mechanical properties significantly influences the displacement response. Furthermore, the displacements are smaller (in magnitude) for $L/h=10$ compared to $L/h=5$, which suggests that increasing the slenderness of the beam reduces the normalized displacements.

4. Conclusions

This study investigated the mechanical behavior of a cantilever functionally graded material (FGM) beam subjected to combined shear and bending loads. A novel elastic modulus formulation including two gradation parameters was introduced to represent both the material gradation and the longitudinal modulus ratio. Three types of mechanical property distributions across the beam thickness were analyzed: the classical model, new model-1 (with properties varying from the outer metal surface to the inner ceramic core), and new model-2 (with properties varying from the outer ceramic surface to the inner metal core). The main findings are summarized as follows:

1. The material property distribution has a significant influence on the normal stress σ_{xx} and the normalized displacement \bar{v} , while its effect on the shear stress τ_{xy} remains relatively limited.
2. New model-1 generally predicts lower normal stresses and displacements compared to the classical model and new model-2.
3. Increasing the length-to-thickness ratio L/h leads to a significant increase in normal stress σ_{xx} and a decrease in the normalized displacement \bar{v} .
4. The shear stress τ_{xy} follows a parabolic distribution across the thickness, with maximum values at the mid-thickness for new models-1 and -2, and slightly shifted toward the upper surface in the classical model.

References

1. Reddy, J. (2000). Analysis of functionally graded plates. *International Journal for Numerical Methods in Engineering*, 47(1-3), 663-684. [https://doi.org/10.1002/\(SICI\)1097-0207\(20000110/30\)47:1/3<663::AID-NME787>3.0.CO;2-8](https://doi.org/10.1002/(SICI)1097-0207(20000110/30)47:1/3<663::AID-NME787>3.0.CO;2-8).
2. Chakraborty, A., Gopalakrishnan, S., Reddy, J. (2003). A new beam finite element for the analysis of functionally graded materials. *International Journal of Mechanical Sciences*, 45(3), 519-539. [https://doi.org/10.1016/S0020-7403\(03\)00058-4](https://doi.org/10.1016/S0020-7403(03)00058-4).
3. Rizov, V.I., Altenbach, H. (2025). Effect of spatial translational motion on lengthwise fracture in functionally graded beams. *Advances in Aircraft and Spacecraft Science*, 12(2), 161-175. <https://doi.org/10.12989/aas.2025.12.2.161>.
4. Şimşek, M., Reddy, J. (2013). Bending and vibration of functionally graded microbeams using a new higher order beam theory and the modified couple stress theory. *International Journal of Engineering Science*, 64, 37-53. <https://doi.org/10.1016/j.ijengsci.2012.12.002>.
5. Zohra, A., Rabia, B., Tahar, H.D. (2024). Study and analysis of porosity distribution effects on the

- buckling behavior of functionally graded plates subjected to diverse thermal loading. *Coupled Systems Mechanics*, 13(2), 115-132. <https://doi.org/10.12989/csm.2024.13.2.115>.
6. Ghelamallah, R., Rabia, B., Youcef, T., Tahar, H.D. (2025). Vibration analysis of FG beams with a new type of gradient variation reposed on elastic foundations. *Structural Engineering and Mechanics*, 95(4), 327-340. <https://doi.org/10.12989/csm.2025.14.2.183>.
 7. Daikh, A., Djedidi, O., Allali, O., Belarbi, M.O., Nadji, L., Houari, M.S.A., ... Abdraboh, A.M. (2025). Buckling of functionally graded porous metal foam nanoshells. *Structural Engineering and Mechanics*, 94(5), 363-374. <https://doi.org/10.12989/sem.2025.94.5.363>.
 8. Adim, B., Daouadji, T.H., Mekid, R. (2025). Analysis of the mechanical behavior of functionally graded plates: Effect of boundary conditions and micromechanical models. *Structural Engineering and Mechanics*, 95(1), 31-42. <https://doi.org/10.12989/sem.2025.95.1.031>.
 9. Akbas, S.D. (2020). Dynamic analysis of a laminated composite beam under harmonic load. *Coupled Systems Mechanics*, 9(6), 563-573. <https://doi.org/10.12989/csm.2020.9.6.563>.
 10. Daouadji, T.H. (2017). Analytical and numerical modeling of interfacial stresses in beams bonded with a thin plate. *Advances in Computational Design*, 2(1), 57-69. <https://doi.org/10.12989/acd.2017.2.1.057>.
 11. Henni, A.H., Daouadji, T.H. (2025). Analysis and modeling of the behavior of exponentially graded cantilever beams loaded by various parabolic distribution loads. *Structural Engineering and Mechanics*, 95(1), 43-50. <https://doi.org/10.12989/sem.2025.95.1.043>.
 12. Adim, B., Daouadji, T.H., Bekda, K. (2025). Micromechanical model-based analysis of porous functionally graded plates behavior using refined higher-order theory. *Advances in Aircraft and Spacecraft Science*, 12(2), 95-115. <https://doi.org/10.12989/aas.2025.12.2.095>.
 13. Daouadji, T.H. (2013). Analytical analysis of the interfacial stress in damaged reinforced concrete beams strengthened by bonded composite plates. *Strength of Materials*, 45(5), 587-597. <https://doi.org/10.1007/s11223-013-9496-4>.
 14. Hung, C.C., Nguyen, T. (2023). Aviation stability analysis with coupled system criterion of theoretical solutions. *Coupled Systems Mechanics*, 12(3), 221-239. <https://doi.org/10.12989/csm.2023.12.3.221>.
 15. Rizov, V.I. (2021). Delamination analysis of multilayered beams exhibiting creep under torsion. *Coupled Systems Mechanics*, 10(4), 317-331. <https://doi.org/10.12989/csm.2021.10.4.317>.
 16. Raundal, M.S., Dhepe, S.N., Bambole, A.N., Ghugal, Y.M. (2025). Exact elasticity solution of functionally graded beam subjected to transverse loads. *Structural Engineering and Mechanics*, 94(2), 129-141. <https://doi.org/10.12989/sem.2025.94.2.129>.
 17. Zohra, A., Benferhat, R., Tahar, H.D., Tounsi, A. (2021). Analysis on the buckling of imperfect functionally graded sandwich plates using new modified power-law formulations. *Structural Engineering and Mechanics*, 77(6), 797-807. <http://doi.org/10.12989/sem.2021.77.6.797>.
 18. Benferhat, R., Daouadji, T.H., Abderezak, R. (2021). Effect of porosity on fundamental frequencies of FGM sandwich plates. *Composite Materials and Engineering*, 3(1), 25. <http://doi.org/10.12989/cme.2021.3.1.025>.
 19. Aicha, K., Rabia, B., Daouadji, T.H., Bouzidene, A. (2020). Effect of porosity distribution rate for bending analysis of imperfect FGM plates resting on Winkler-Pasternak foundations under various boundary conditions. *Coupled Systems Mechanics*, 9(6), 575-597. <http://doi.org/10.12989/csm.2020.9.6.575>.
 20. Rabia, B., Tahar, H.D., Abderezak, R. (2020). Thermo-mechanical behavior of porous FG plate resting on the Winkler-Pasternak foundation. *Coupled Systems Mechanics*, 9(6), 499-519. <http://doi.org/10.12989/csm.2020.9.6.499>.
 21. Sankar, B.V. (2001). An elasticity solution for functionally graded beams. *Composites Science and Technology*, 61(5), 689-696. [https://doi.org/10.1016/S0266-3538\(01\)00007-0](https://doi.org/10.1016/S0266-3538(01)00007-0).
 22. Zhong, Z., Yu, T. (2007). Analytical solution of a cantilever functionally graded beam. *Composites Science and Technology*, 67(3-4), 481-488. <https://doi.org/10.1016/j.compscitech.2006.08.023>.
 23. Filippi, M., Carrera, E., Zenkour, A.M. (2015). Static analyses of FGM beams by various theories and finite elements. *Composites Part B: Engineering*, 72, 1-9. <https://doi.org/10.1016/j.compositesb.2014.12.004>.

24. Alimoradzadeh, M., Akbaş, Ş.D. (2022). Nonlinear thermal vibration of FGM beams resting on nonlinear viscoelastic foundation. *Steel and Composite Structures*, 44(4), 557-567. <https://doi.org/10.12989/scs.2022.44.4.557>.
25. Adim, B., Daouadji, T.H. (2024). Analysis of the hygro-thermo-mechanical response of functionally graded plates resting on elastic foundations based on various micromechanical models. *Geomechanics & Engineering*, 38(4), 409-420. <https://doi.org/10.12989/gae.2024.38.4.409>.
26. Bennai, R., Ait Atmane, R., Bernard, F., Nebab, M., Mahmoudi, N., Ait Atmane, H., ... Tounsi, A. (2022). Study on stability and free vibration behavior of porous FGM beams. *Steel and Composite Structures*, 67-82. <https://doi.org/10.12989/scs.2022.45.1.067>.
27. Yaylacı, M., Yaylacı, E.U., Özdemir, M.E., Öztürk, Ş., Sesli, H. (2023). Vibration and buckling analyses of FGM beam with edge crack: finite element and multilayer perceptron methods. *Steel and Composite Structures*, 46(4), 565-575. <https://doi.org/10.12989/scs.2023.46.4.565>.
28. Khorasani, M., Lampani, L., Tounsi, A. (2022). A refined vibrational analysis of the FGM porous type beams resting on the silica aerogel substrate. *Steel and Composite Structures*, 633-644. <https://doi.org/10.12989/scs.2023.47.5.633>.
29. Tlidji, Y., Benferhat, R., Tahar, H.D. (2024). Investigating the influence of porosity distribution rates on free vibration of FG beams utilizing state space method. *Structural Engineering and Mechanics*, 92(5), 463-471. <https://doi.org/10.12989/sem.2024.92.5.463>.
30. Guendouz, I., Khebizi, M., Guenfoud, H., Guenfoud, M., El Fatmi, R. (2022). Analysis of torsional-bending FGM beam by 3D Saint-Venant refined beam theory. *Structural Engineering and Mechanics*, 84(3), 423-435. <https://doi.org/10.12989/sem.2022.84.3.423>.
31. Saghafi, H., Alibeigloo, A. (2025). Static and vibration analysis of sandwich beam with FGM core and viscoelastic interface using differential quadrature method. *Structural Engineering and Mechanics*, 94(3), 171-186. <https://doi.org/10.12989/sem.2025.94.3.171>.
32. Hosseini, S.A.H., Rahmani, O., Refaiejad, V., Golmohammadi, H., Montazeripour, M. (2023). Free vibration of deep and shallow curved FG nanobeam based on nonlocal elasticity. *Advances in Aircraft and Spacecraft Science*, 10(1), 51. <https://doi.org/10.12989/aas.2023.10.1.051>.
33. Candaş, A., Oterkus, E., İmrak, C.E. (2024). Ordinary state-based peridynamic modelling of crack propagation in functionally graded materials with micro cracks under impact loading. *Mechanics of Advanced Materials and Structures*, 31(30), 13502-13517. <https://doi.org/10.1080/15376494.2023.2287180>.
34. Siam, O.A., Shanab, R.A., Eltaher, M.A., Mohamed, N.A. (2023). Free vibration analysis of nonlocal viscoelastic nanobeam with holes and elastic foundations by Navier analytical method. *Advances in Aircraft and Spacecraft Science*, 10(3), 257-279. <https://doi.org/10.12989/aas.2023.10.3.257>.
35. Candaş, A., Oterkus, E., İmrak, C.E. (2023). Peridynamic simulation of dynamic fracture in functionally graded materials subjected to impact load. *Engineering with Computers*, 39(1), 253-267. <https://doi.org/10.1007/s00366-021-01540-2>.
36. Bouazza, M., Amara, K., Zidour, M. (2024). Employing an analytical method for post-buckling analysis of functionally graded beams. *Advances in Aircraft and Spacecraft Science*, 11(4), 299-310. <https://doi.org/10.12989/aas.2025.11.4.299>.
37. Hacıoğlu, A., Candaş, A., Baykara, C. (2023). Large deflections of functionally graded nonlinearly elastic cantilever beams. *Journal of Engineering Materials and Technology*, 145(2), 021002. <https://doi.org/10.1115/1.4056034>.
38. Kablia, A., Benferhat, R., Tahar, H.D. (2022). Dynamic of behavior for imperfect FGM plates resting on elastic foundation containing various distribution rates of porosity: Analysis and modeling. *Coupled Systems Mechanics*, 11(5), 389-409. <https://doi.org/10.12989/csm.2022.11.5.389>.
39. Youzera, H., Meftah, S.A., Tounsi, A., Ghazwani, M.H., Alnujaie, A. (2025). Finite element formulation for free vibration analysis of porous FGM beams under thermal excitation. *Computers and Concrete*, 36(4), 419. <https://doi.org/10.12989/cac.2025.36.4.419>.
40. Benhenni, M.A., Daouadji, T.H., Abbes, B., Abbes, F., Li, Y., Adim, B. (2019). Numerical analysis for free vibration of hybrid laminated composite plates for different boundary conditions. *Structural*

- Engineering and Mechanics, 70(5), 535-549. <https://doi.org/10.12989/sem.2019.70.5.535>.
41. Rabia, B., Daouadji, T.H., Abderezak, R. (2019). Effect of porosity in interfacial stress analysis of perfect FGM beams reinforced with a porous functionally graded materials plate. *Structural Engineering and Mechanics*, 72(3), 293-304. <https://doi.org/10.12989/sem.2019.72.3.293>.
 42. Tayeb, B., Daouadji, T.H. (2020). Improved analytical solution for slip and interfacial stress in composite steel-concrete beam bonded with an adhesive. *Advances in Materials Research*, 9(2), 133-153. <https://doi.org/10.12989/amr.2020.9.2.133>.
 43. Tahar, H.D., Boussad, A., Abderezak, R., Rabia, B., Fazilay, A., Belkacem, A. (2019). Flexural behaviour of steel beams reinforced by carbon fibre reinforced polymer: Experimental and numerical study. *Structural Engineering and Mechanics*, 72(4), 409-420. <https://doi.org/10.12989/sem.2019.72.4.409>.
 44. Zohra, A., Rabia, B., Tahar, H.D. (2023). Critical thermal buckling analysis of porous FGP sandwich plates under various boundary conditions. *Structural Engineering and Mechanics*, 87(1), 29-46. <https://doi.org/10.12989/sem.2023.87.1.029>.
 45. Loy, C.T., Lam, K.Y., Reddy, J.N. (1999). Vibration of functionally graded cylindrical shells. *International Journal of Mechanical Sciences*, 41(3), 309-324. [https://doi.org/10.1016/S0020-7403\(98\)00054-X](https://doi.org/10.1016/S0020-7403(98)00054-X).